Implications of decadal to century scale glacio-hydrological change for water resources of the Hood River Basin, OR U.S.A.

Chris Frans[1], Erkan Istanbulluoglu[1], Dennis P. Lettenmaier[2], Garry Clarke[3], Theodore J. Bohn[4], Matt Stumbaugh[1]

[1]Department of Civil and Environmental Engineering, University of Washington, Seattle, WA, USA
[2]Department of Geography, University of California, Los Angeles, CA, USA
[3]Department of Earth, Ocean, and Atmospheric Sciences, University of British Columbia, Vancouver, BC, Canada
[4]School of Earth and Space Exploration, Arizona State University, Tempe, AZ, USA

Corresponding Author:
Chris Frans
Department of Civil and Environmental Engineering
University of Washington
Box 352700
Seattle, WA 98195
chrisf2@uw.edu

Abstract

In glacier fed rivers melting of glacier ice sustains streamflow during the driest times of the year, especially during drought years. Anthropogenic and ecologic systems that rely on this glacial buffering of low flows are vulnerable to glacier recession as temperatures rise. We demonstrate the evolution of glacier melt contribution in watershed hydrology over the course of a 184-year period from 1916-2099 through the application of a coupled hydrological and glacier dynamics model to the Hood River Basin in Northwest Oregon, U.S.A. We performed continuous simulations of glaciological processes (mass accumulation and ablation; lateral flow of ice; heat conduction through supra-glacial debris) which are directly linked with seasonal snow dynamics as well as other key hydrologic processes (e.g., evapotranspiration; subsurface flow). Our simulations show that historically, the contribution of glacier melt to basin water supply was up to 79% at upland water management locations. We also show that supraglacial debris cover on the Hood River glaciers modulates the rate of glacier recession and progression of dry season flow at upland stream locations with debris covered glaciers. Our model results indicate that dry season (July-Sept.) discharge sourced from glacier melt started to decline early in the 21st century following glacier recession that started early in the 20th century. Changes in climate over the course of the current century will lead to 14-63% (18-78%) reductions in dry season discharge across the basin for IPCC emission pathway RCP4.5 (RCP8.5). The largest losses will be at upland drainage locations of water diversions that were dominated historically by glacier melt and seasonal snowmelt. The contribution of glacier melt not only varies greatly in space, but also in time. It displays a strong decadal scale fluctuations that are super-imposed on the effects of a long-term climatic warming trend. This decadal variability results in reversals in trends in glacier melt which underscore the importance of long time series of glacio-hydrologic analyses for evaluating the hydrological response to glacier recession.

1. Introduction

Mountain glaciers provide an important source of water in climates with highly seasonal precipitation patterns as snow and ice masses in partially glacierized watersheds redistribute wet season precipitation to streamflow at times of the year where there are few other sources of water entering streams (Meier, 1969; Fountain and Tangborn, 1985; Barnett et al., 2005). During dry and warm years when seasonal snow accumulation is reduced, the contribution of glaciers to low flows is further amplified as a larger area of glacier surfaces is exposed to melt for longer durations of the year (Fleming and Clarke, 2005) . As the climate warms, this natural buffering of low flows provided by glaciers is expected to increase initially; however reductions in glacier area will eventually overcome enhanced rates of melting from warmer temperatures (Hock et al., 2005; Moore et al., 2009; Baraer et al., 2012). The timescales at which increased ablation from climate warming augments streamflow and the rate of declines after a peak in augmentation are not well understood. Observational records of discharge downstream from glaciers are often not long enough to identify these peaks. Furthermore, these phases of response to a positive trend in temperature may become less distinct over short time intervals as they can be superimposed on streamflow patterns linked to natural decadal climate variability (e.g., Beebee and Manga, 2004).

Previous research by Nolin et al., 2010; Pelto, 2011; Pelto, 2008; Moore and Demuth, 2001; Stahl and Moore, 2006; Stahl et al. 2008; and Jost et al. 2012 has diagnosed the contribution of glacier melt to streamflow in several partially glacierized river basins in western North America. Most of these studies etiher/or a) have analyzed relatively short observation periods (Nolin et al., 2010), b) focus primarily on the glacierized parts of the river basins of interest (Moore and Demuth, 2001; Nolin et al., 2010), c) do not differentiate seasonal snowmelt and glacier ice melt (Stahl and Moore, 2006; Nolin et al., 2010), or d) use water balance methods that simplify or do not consider the non-glacierized portions of the watersheds of interest (Pelto, 2008; 2011). More recently model applications that simulate both hydrologic processes and glacier mass with varying degrees of complexity have been used to describe the glacier melt contribution to streamflow (e.g., Jost et al., 2012; Stahl et al., 2008; Naz et al., 2014; Immerzeel et al., 2012; Ragettli and Pellicciotti, 2012). When constrained by and evaluated with local observations, these models allow analyses of processes at spatial and temporal scales that cannot be accomplished with local observations alone. Furthermore, these models can be used to test hypotheses of how a partially glacierized system may respond as the climate continues to warm.

In partially glacierized watersheds where streamflow is utilized for agriculture and domestic uses and where aquatic habitats rely on glacier-driven low flows the following three questions are critical for resource managers: (1) what is the seasonal contribution of glaciers to streamflow through the stream network? (2) how do glaciers respond to climate variability and climate warming? and (3) what is the relationship between glacier melt and streamflow response over time? These questions are important in the Hood River basin of northwestern Oregon (Fig. 1) whose headwaters originate with the glaciers of Mt. Hood. We examine the contribution of glacier melt to streamflow in the Hood River basin at a range of spatial scales for 184 years using a spatially distributed hydrology model coupled with a glacier dynamics model as described in (Naz et al., 2014). To account for the influence of debris on ablation from the glacier surfaces, we incorporate a debris surface energy balance model (DSEB) based on the work of Reid and Brock (2010). In what follows we first describe our study site in greater detail, and follow with a brief description of the modeling framework. We follow with results of our historical reconstructions, and projections of the response of the coupled glacier and hydrologic system through the end of the 21st century.

2. Study Site

The Hood River heads on the northern flanks of Mount Hood, a glaciated stratovolcano that reaches an elevation of 3429 m a.s.l. (North American Vertical Datum of 1988 (NAVD 88)). The Hood River drainage basin (~880 km^2) includes 89 km^2 of mostly irrigated agricultural land, largely consisting of perennial crops (apple and pear orchards and grape vineyards) that have high water demand during summer months. Stream discharge in the basin is managed through multiple flow diversion structures and two small storage reservoirs (5,100,000 m^3 capacity) that provide agricultural water supply to meet seasonal irrigation demands. Irrigation diversions occur from April 15 through September 30, peaking in July or August. In some reaches consumptive diversion during the irrigation season is estimated to be 40% of natural flow (Coccoli, 2002). Reliable irrigation water supply for fruit trees and vines is more critical than for annual herbaceous crops as a deficit of water can not only lead to reduced yields in the current year, but can also reduce yields in subsequent years or result in death of the plants

(Steduto et al., 2012). Furthermore, water deficits can be detrimental beyond the period of peak evapotranspiration as the fruit continues to develop prior to late summer and autumn harvest (Steduto et al., 2012). In addition to irrigation, water in the basin is used for hydropower, potable water supply for a population of 40,000, protection of aquatic species, and recreation.

Many of the agricultural water supply diversion structures are located on streams at high elevations in close proximity to partially glacierized headwater catchments. Glaciers in these upland catchments have retreated up to 60% over the past century (Lillquist and Walker, 2006; Jackson and Fountain, 2007). The fraction of glacier cover in the basin above its outlet at the Columbia River is modest (<1%), however it is as large as 20% in smaller headwater drainages that are located above water diversion locations. The change in area of individual glaciers over the historical period has been highly variable. The two largest glaciers in the Hood River drainage, Eliot and Coe (Fig. 1), have experienced the smallest amounts of areal change which is largely attributed to supra-glacier debris (colluvium) cover on their ablation areas, northerly exposure, and the elevation range of the accumulation areas (Jackson and Fountain, 2007). Debris cover complicates surface energy dynamics and ablation rates of underlying glacier ice as thin layers of debris lower the local albedo and enhance ablation, while continuous thicker layers of debris act as an insulator and retard ablation (e.g., Clark et al., 1994; Conway and Rasmussen, 2000; Mihalcea et al., 2006). While these historical patterns of glacier retreat over the 20th century on Mount Hood have been well documented, the consequences of these changes on streamflow are not known. Moreover, the contribution of glacier melt to streamflow and water resource management across the basin is not fully understood.

3. Methodology

3.1 Hydrological Model

The distributed hydrology soil vegetation model, DHSVM (Wigmosta et al., 1994), served as the modeling foundation for the simulations of hydrological processes across the heterogeneous landscape. DHSVM has been widely applied in mountainous watersheds across the globe, with numerous applications in the Pacific Northwest (e.g., Elsner et al., 2010; Cuo et al., 2011; Jost et al., 2009; Casola et al., 2009). The model provides a physically based representation of snowmelt and evapotranspiration and analytical representations of the routing of surface and subsurface flow based on the distribution of watershed characteristics (topography, vegetation, soil, climate) and physical and analytical parameters over the discretized model domain (Kampf and Burges, 2007). For applications in mountainous areas with complex topography, the more salient components of the model include a surface energy balance (SEB) multilayer snow and ice melt and accumulation model (Andreadis et al., 2009; Naz et al., 2014). To simulate spatial changes in glacier mass and area, a representation of glacier dynamics (Clarke et al., 2015) is integrated into the hydrological modeling framework (Naz et al., 2014).

The ablation areas of the Eliot and Coe glaciers (Fig. 1), the two largest glaciers in the basin, are partially covered with a layer of colluvial debris. To account for the influence of debris on ablation rates we have integrated algorithms based on the debris covered glacier DSEB model of Reid and Brock (2010) that solves the subsequent energy balance equations vertically with fine scale vertical node spacing. The debris surface temperature (T_s) is iteratively calculated to balance the energy fluxes at the atmosphere-debris interface considering the temperature of the atmosphere (T_a, at 2 m) and underlying debris (T_d),

$$SW_{net} + LW_{in} + LW_{out}(T_s) + H(T_s,T_a) + LE(T_s,T_a) + G(T_s,T_d) + P(T_s,T_a) = 0 \quad (1)$$

where SW_{net} is net shortwave radiation, LW_{in} is incoming longwave radiation, LW_{out} is outgoing longwave radiation, H is sensible heat flux, LE is the latent exchange, G is the flux of heat to subsurface debris layers, and P is the energy advected from liquid precipitation. Equation 1 is linked with the internal temperature profile within the debris layer ($T_d(z,t)$) through the conductive surface heat flux term (G), and is modeled by calculating conductive heat fluxes through the debris,

$$\rho c \frac{\partial T_d(z,t)}{\partial t} = \frac{\partial}{\partial z}\left(k_{debris} \frac{\partial T_d(z,t)}{\partial z}\right) \quad (2)$$

where ρ, c, and k_{debris} are the density, specific heat capacity and the effective thermal conductivity of the debris. The total thickness of the debris is discretized into N computational nodes with vertical spacing dz. To determine ablation rates, the conductive heat flux at the lower boundary, the debris-ice interface, is calculated as,

$$G_{ice} = k_{debris} \frac{T_d(N-1) - T_f}{dz} \quad (3)$$

where G_{ice} is the conductive heat flux to the underlying ice, $T_d(N-1)$ is the temperature of the debris at the computation node above the debris-ice interface, and T_f is the temperature of the debris-ice interface (assumed to be constant at $0°$ C). The algorithms as implemented are consistent with Reid and Brock (2010) with the exception of the numerical method of estimating surface temperature. Where Reid and Brock (2010) used the Newton-Raphson technique, we use the Brent method (Brent, 1973) to reduce computation time. Additionally for computational stability we discretized the debris layer into 20 vertical computational nodes for all model debris covered grid cells, regardless of total debris thickness. We ran the model at a 3-hour time step to account for diurnal scale fluctuations of surface energy dynamics of snow, debris surface, and ice, all of which affect the net energy exchange of the surfaces of snow and ice at longer time scales. We used the 3-hour time step for all hydrological computations, even though some processes, such as streamflow generation at seasonal time scales may not require this fine temporal resolution. We evaluated the ability of our model to reproduce historic observed streamflow at both daily and monthly time scales.

3.2 Data

The model is forced with meteorological data at 3 hour intervals. The meteorological forcing data consist of precipitation, air temperature, relative humidity, wind speed, downwelling longwave radiation, and downward shortwave radiation. We use a gridded dataset generated using observed daily minimum and maximum temperature, accumulated precipitation, and mean wind speed that have been interpolated from NOAA Cooperative Observing Network (Co-Op) weather stations to a 1/16 degree spatial resolution (~6 km) using the methods of Hamlet and Lettenmaier, (2005). Using these methods the data are adjusted so that long term trends are consistent with those observed at stations of the NOAA Global Historical Climatology Network (GHCN-D) which are of the highest quality and have been corrected for any introduction of biases from changes in station location and instrumentation, among others. Additionally, the data are scaled to be consistent with the climatology of the Parameter-elevation Regressions on Independent Slopes Model data (PRISM, version 3) which accounts for finer spatial scale variability imposed by complex topography (Daly et al., 1994). Hamlet and Lettenmaier (2005) provide a complete description of this methodology. The Mountain Microclimate Simulation model (MTCLIM; Thornton and Running, 1999), as implemented by Bohn et al. (2013), is used to disaggregate these variables to sub-daily time intervals and to estimate the other required meteorological variables (shortwave radiation, longwave radiation, relative humidity). In DHSVM the input meteorological variables are further interpolated to the model resolution (90 meters) using elevation gradients (temperature, precipitation) and seasonal and diurnally varying scaling to represent the influence of topography on solar radiation.

Geospatial input data required by the model include elevation, vegetation classification, soil texture classification, initial glacier ice thickness, and supraglacial debris thickness. Digital elevation model (DEM) data at 30 m. spatial resolution were obtained from the United States Geological Survey (USGS; ned.usgs.gov/). Vegetation classification was specified using the National Land Cover Database (NLCD 2001; www.mrlc.gov/nlcd2001.php). Soil classification data from the Natural Resource Conservation Service (NRCS) soil database (SSURGO; http://websoilsurvey.nrcs.usda.gov/) and the Soil Resource Inventory (SRI) were used to define soil texture classifications across the basin. All data were resampled (bilinearly) to 90 meter spatial resolution for consistency. Parameters for each vegetation class (leaf area index, rooting depth, stomatal resistance) and soil texture (porosity, lateral conductivity, field capacity) were taken from previous DHSVM applications in the region and adjusted during model calibration as needed. Glacier bed topography, the elevation of the land surface beneath the glacier ice was estimated using the method of Clarke et al. (2013). Supraglacial debris thickness on Eliot glacier was interpolated to the model grid resolution from point measurements (Jackson, 2007). No measurements of debris thickness are available for Coe glacier, thus aerial imagery archived in Google Earth was used to identify debris extent and the longitudinal gradient in debris thickness observed on Eliot glacier was used to estimate the distribution of debris thickness. The thickness of the debris at each model element was assumed to be constant in time.

A multistep spin-up procedure was used to estimate the initial distribution of ice thickness early in the 20th century. In this procedure the glacier dynamics model that simulates ice movement through creep (offline from the hydrological model) is forced with a temporally constant spatially distributed surface mass balance field so that the modeled steady state ice extent closely matches historical estimates. Due to the lack of knowledge of historical ice thicknesses this method assumes that if the extent simulated using glacier dynamics matches the observed extent, it provides an accurate estimate of the distribution of ice thickness at the time of observation. This assumption is tested by comparing modeled and observed rates of recession during the historical period of analysis. Furthermore, using the glacier dynamics model to spin-up the glaciers provides a distribution of ice that is mechanistically stable. Frans et al. (2015) provide a more detailed description of this methodology. Area estimates provided in Jackson and Fountain (2007) were used to delineate the historical extent.

We used output of general circulation models (GCMs) from the Coupled Model Inter-Comparison Project 5 (CMIP5, Taylor et al., 2012) to project glacier and hydrologic conditions through the end of the 21st century. Projections of 9 GCMs (Table 2) selected based on the PNW model skill rankings of Rupp et al. (2013) and available climate variables of representative concentration pathway scenarios RCP4.5 and RCP8.5 were used. Daily maximum and minimum temperature, and precipitation and wind speed from the GCM output were downscaled to 1/16 degree spatial resolution using the Multivariate Adaptive Constructed Analogs (MACA) statistical downscaling method (Abatzoglou and Brown, 2012). Generation of the sub-daily meteorological forcing data follows the methods previously outlined for the historical data.

3.3 Model Testing

Following Konz and Seibert (2010) and Finger et al. (2011) we calibrated and evaluated our glacio-hydrological model using historical observations of both hydrological and glaciological variables. We compared our simulations with observations and estimates of glacier extent, measurements of glacier ablation under debris, oxygen isotope analyses, and discharge observations. Given the relatively small agricultural portion of the basin, and our broader focus on glacier melt contribution during dry season over the extended period 1916-2099 (184 years), we used naturalized flows (the flows that would have occurred absent the effects of water management) at the Hood River at Tucker bridge (USGS 14120000) for model calibration; we did not attempt to model the effects of water management throughout the basin. Using naturalized flows also allowed us to focus on only the influence of climate on glacio-hydrology (the signature of water management operations are inherently uncertain both historically and in the future). At the West Fork Hood River near Dee (USGS gauge 14118500) agricultural impacts on streamflow are minor and we did not have access to naturalized flows. Guided by comparisons of our model predictions with observations we adjusted selected calibration parameters accordingly. Key parameters that we calibrated include the precipitation elevation gradient, glacier albedo, maximum snow albedo used in temporal decay curves, the effective thermal conductivity of supraglacial debris, and soil characteristics.

The different sources of data we used for model testing vary in the spatial scale they represent (e.g., point ablation measurements, basin integrated discharge) as well as temporally with different observation intervals and periods of record. For example, glacier area estimates are available for two years (1904 and 2004); estimates of ablation below debris are available for a single melt season; and naturalized daily discharge is available for 10 years. Due to the spatial and temporal inconsistencies among the different data sets available to us for model evaluation, we calibrated the model manually, via comparison of model-predicted glacier-related variables as well as streamflow. Various studies (e.g., Konz and Seibert, 2010; Finger et al., 2011) have shown that parameter uncertainty and equifinality issues can be greatly reduced when multiple variables are used in the calibration process. In this study we have not further explored equifinality issues, however we note that in a previous study that used the same model in a somewhat narrower application (Naz et al., 2014) we did so, and many of the insights developed there are applicable to this study as well.

We adjusted and calibrated soil parameters (lateral hydraulic conductivity, soil depth) and the parameters that control the spatial distributions of meteorological forcings (temperature and precipitation lapse rates) to match modeled streamflow to daily and seasonal naturalized discharge at the Hood River at Tucker Bridge, located close basin outlet, and observed streamflow at an upstream location at the West Fork of the Hood River near Dee, where the impact of irrigation is negligible (Fig. 1). Snow albedo, glacier albedo and the effective thermal conductivity of debris were adjusted to match glacier area and point scale ablation rates. Because the glaciers only cover ~1% of the basin area, the effects of glacier parameters on streamflow were minimal within the time scales of streamflow calibration for gauges with observations which are located in the lower portion of the basin.

As is common in hydrologic model applications, we do not represent the impacts of water management on streamflow, both because the effects of water management operations are inherently uncertain, and because the model predicts the streamflows that would have occurred absent water management, hence it makes more sense to remove water management effects from the observations (e.g., by adjusting for observed changes in reservoir storage and observed irrigation diversions and return flows) rather than developing a separate water management model. Naturalized discharge was estimated from measurements and known water management operations by the United States Bureau of Reclamation (USBR; www.usbr.gov/pn/programs/studies/oregon/hoodriver/index.html) at the Hood River at Tucker Bridge USGS gauging station (Fig. 1) for water years 2002-2011. USBR estimated naturalized discharge by adding water diverted by irrigation districts and municipalities for potable water, seasonal filling of two small reservoir systems and by subtracting seasonal reservoir drawdowns and return flow from irrigation districts to the observed discharge. The reader is referred to the above web site for details of their procedures.

4. Results

4.1 Model Evaluation

The Nash Sutcliffe Efficiency (NSE) coefficients for modeled daily and monthly mean streamflow discharge were 0.61 and 0.78 at the main stem of the Hood River at Tucker Bridge (2002-2011); and 0.56 and 0.82 at the West Fork of the Hood River near Dee (1933-2011). Modeled and observed streamflow at both locations are shown in Figure 2. Both monthly and daily NSE values are typical of hydrological model applications in topographically complex regions where model forcings are estimated by relatively sparse networks (or precipitation in particular). We also note that the NSE values are dominated by high runoff events and seasons, and hence while they provide evidence of plausible model performance, they do not shed much light on the low flow seasons which are the focus of this paper (because the glacier contributions to streamflow are highest then). We did explore alternate model parameter combinations that improved NSE, but generally these had the effect of degrading low flow performance. Model performance generally is best during the melt season recession and low flow periods, which are the time of year that is critical for water resource management, and when the glacier contribution is most important. The model underestimates September discharge slightly, which may be attributed to a model deficiency in simulating deep subsurface flow and uncertainty in the estimation of naturalized discharge. The final set of model parameters are reported in Table 1.

4.2 Defining Glacier Melt Contribution to Discharge

A critical first step in assessing the role of glaciers in catchment hydrology is to define how the glacier contribution to streamflow discharge is quantified. Glacier contribution to streamflow has generally been defined either as all water leaving the glacier covered area (including direct flow from rain and snowmelt) or the melting of glacier ice only (see La Frenierre and Mark, 2014). Nolin et al. (2010) conducted a geochemical isotopic mixing analysis of the Middle Fork of the Hood River to determine the relative contribution of glaciers to stream discharge. Samples of discharge from the glacier terminus, groundwater from downstream areas outside of the glaciers, and discharge from a stream location where these two sources are mixed were used in the analysis. In their approach, all water leaving the glacier footprint is lumped as glacier melt. To facilitate comparison with these estimates, we plot the ratio of the modeled discharge leaving the footprint of the Eliot glacier to total discharge modeled downstream in Eliot Creek (Fig. 3) above the confluence with the Middle Fork (Fig. 1). The dates and locations are consistent with those sampled during WY 2007 by Nolin et al. (2010). For the sequence of the three sampling dates, the method of Nolin et al. found the glacier contribution to be 88$\pm$4, 78$\pm$3, and 76$\pm$3% at a single sampling time on each day. For these dates the model simulated the diurnal range of glacier contribution to be 74-95, 75-92, and 58-76%. The geochemically derived estimates fall within in these modeled ranges for the corresponding sampling dates (Fig. 3).

Modeled discharge derived only from the melting of glacier ice is also plotted (excluding snowmelt, rain); highlighting the differences between the two definitions of glacier melt contribution. During the period before Sept. 15 the mean contribution from the glacier footprint is 84% while the contribution from the melting of only glacier ice is 60%. The relative glacier contribution from these two definitions diverges the most after mid-September when autumn rainfall and transient snowmelt increases, outweighing the contribution of glacier ice melt (Fig. 3). In the analyses we report in the remainder of this article, we take the glacier contribution to discharge as melting of glacier ice only; we do not include snowmelt and rain on the glaciers. These seasonal sources of water will still contribute to runoff generation after a glacier has receded. Limiting the definition of the glacier contribution to only include the melting of glacier ice is more appropriate to long-term water management considerations, as it does not include fluxes of water that will still be present in a non-glacierized state.

We conducted a parameter sensitivity analysis to quantify how the selection of key model parameters used in model calibration can influence the modeled relative contribution of glacier melt to streamflow. We defined parameter sensitivity as:

$$\alpha = \frac{\dfrac{C_0 - C_i}{\frac{1}{2}\left(C_0 + C_i\right)}}{\dfrac{\theta_0 - \theta_i}{\frac{1}{2}\left(\theta_0 + \theta_i\right)}} \qquad (4)$$

The sensitivity (α) is reported as a percent change in glacier melt contribution (C) per (one) percent change in the parameter value (θ). θ_0 is taken as the calibrated value where, θ_i represents an incremental perturbation of the parameter around the calibrated value. Three values of each parameter ($i = 1-3$) were used to calculate sensitivities and identify non-linear patterns of response within the parameter space tested. These values represent the parameter space around the calibrated value, not the entire plausible range. The parameters and values analyzed, and the sensitivities of glacier melt contribution to September and July-September discharge volumes (taken as the modeled mean values for the period of 1916-2010) are reported in Table 3. In general the modeled contribution of glacier melt to total discharge has low sensitivity to parameter selection; however it is sensitive to the value selected for maximum snow albedo used in the snow albedo decay formulation. This parameter influences the rate of melt of the seasonal snowpack that overlies glacier ice, hence it has strong control over the amount of time that glacier ice is exposed to the atmosphere to melt. The sensitivity is greater for the July-September period than for September alone because much of the seasonal snowpack is often melted by September. Increasing this parameter leads to a non-linear decrease in the glacier contribution to runoff. Hence, when selecting this parameter it is important to use available local observations of discharge, glacier ablation, and geochemical analyses where available (section 3.3) to reduce uncertainty in the model estimate of glacier contribution.

4.3 Historical Contribution of Glacier Melt to Discharge

Figure 4 shows modeled mean monthly hydrologic fluxes aggregated across the basin over the period 1916-2005. The largest input of water in the basin is in the form of snowmelt. This occurs during the wet season (November to March) in the form of transient snowmelt at low to mid elevations. During spring and summer (April to September) seasonal snowmelt occurs, gradually decreasing through the dry season. Rainfall occurs throughout the year with a maximum flux in Autumn (September to November) before temperatures decrease and lead to a transition to (mostly) snow in the winter. Potential evapotranspiration calculated for a short reference crop (alfalfa, PETref) and modeled evapotranspiration (ET) follow the seasonal cycle of solar radiation. Irrigation is not represented in the model; hence, actual evapotranspiration is higher than modeled. At the scale of the entire basin the flux from the melting of glacier ice is the smallest input. However, the glacier melt season (JAS) starts when rainfall is at its minimum, snowmelt is minimum, and moisture limitation is maximum (as indicated by the difference between PET and ET).

To obtain a more detailed perspective on the importance of glacier melt, we identify its relative contribution to stream discharge across the basin. Figure 5 shows the modeled mean total discharge and mean glacier melt discharge by day of year over the historical model time period 1916-2005. Also included in the figure is the maximum glacier melt discharge modeled on each day of the year over this time period. As for basin scale discharge patterns (Fig. 5a), the role of glacier melt at the outlet of the basin is modest; on average the maximum contribution of glacier melt is about 7% during September. However, during dry and warm years the contribution is as high as 24%. The contribution of glacier melt is much larger at upstream locations, with the strongest influence at the Eliot Creek diversion location (Fig. 1) where glacier melt contributes up to 54% of daily discharge on average (1916-2005), and is as high as 79% (Fig. 5f), which occurred in Sept. 1924. Historically, dry and warm years (1924, 1977, 1987, 1991, 1994, and 2001) lead to the highest glacier melt contributions. The meteorological data is less reliable during early in the period of analysis due to a reduced number of meteorological observation stations; however the high contribution in 1924 is probable as the glacier state was responding to warm dry PDO phase and adjusting away from the state at end of the last little ice age (*Jackson and Fountain*, 2007).

4.4 The role of debris cover on glacier ablation and retreat

Incorporation of algorithms that represent energy dynamics of supra-glacier debris cover into our model allows us to identify the role of surface debris cover on ablation. Jackson and Fountain (2007) measured ice melt throughout a melt season on the ablation area of Eliot glacier with ablation stakes. We compared our modeled ablation at every grid cell with debris cover between 9/24/2004 and 7/28/2005 with the measurements of Jackson and Fountain (2007) (Figure 6). The model has a roughly exponential decay of ablation with increasing thickness of debris overlying the ice, consistent with the observations. This demonstrates the insulating effects of debris cover. The modeled ablation is more variable than the observations, probably in part because the model domain extends into areas that are often shadowed by the surrounding terrain, and are generally not represented by the observations. To ensure that the model replicated the observed pattern, the constant for the effective thermal conduction of the debris layer (k_{debris}, equations 2 and 3) was adjusted iteratively while all other constants remained fixed (Section 3.1).

To demonstrate the role of debris cover on the response of glacier area, we ran the DHSVM/glacier dynamics model combination for the historical (1916-2005) period. Figures 7a and 7b show ice thickness with and without the representation of debris and its role on the SEB at the end of 2004. In Figures 7a and 7b, the initial model extent is the glacier extent that was used as an initial condition in the model simulations, which was determined through model spinup (Section 3.2). The observation-derived glacier area estimates of Jackson and Fountain (2007) are shown for ~1904 and 2004. The figures demonstrate how the presence of debris cover on Eliot and Coe glaciers reduced the glaciers' sensitivities to warming and slowed their overall retreat. We show the relative significance of the debris-modulated rate of retreat to stream discharge by plotting the ratio of September total discharge volume (Q_{tot}) modeled at the Eliot creek diversion location (located downstream of Eliot glacier) without debris to the simulation with debris (panel c). In the case of no debris, higher ablation rates lead to higher discharge early in the time period and faster recession (panel b) which results in more rapid declines in September discharge volumes. A threshold in glacier area is reached at about 1958 when the higher rate of ablation per unit area of the debris free condition is overcome by the reduction of area through recession. In the last decade of the period discharge is 14% lower in the no debris cover condition.

A key assumption of these model-based analyses is that the debris thickness varies in space however is constant throughout the entire time period. Local debris thickness will vary as surface colluvium melts out of the ice, is deposited from erosion of adjacent slopes, and as the surface of the ice moves. Debris thickness may increase in time with increasing temperature as melting increases. We use the thicknesses measured in 2004 throughout the entire period because historical debris thicknesses are not known. Shallower thicknesses of debris earlier in the century would have increased the rate of retreat by allowing more ablation.

4.5 Projected long-term glacio-hydrological change: 1916 – 2099

To analyze long term glacio-hydrological change and infer future evolution of the Hood river system, we extended our period of analysis through 2099 using time series of future meteorological data statistically downscaled from 9 general circulation models for two emissions pathway scenarios (Section 3.2). Projected seasonal changes in mean annual temperature and precipitation are plotted in Figure 8 (b,c) and seasonal changes are summarized in Table 4. This long period of analysis allows us to explore glacio-hydrological trends in response to warming temperatures. For reference the annual mean PDO index is shown in panel a with red indicating a positive phase (warm, dry) and blue a negative phase (cool, wet). The lengthy period of analysis helps to avoid confounding long-term trends with this low frequency multi-decadal variability that complicates interpretation of shorter time series.

Figs. 8d-e show the relative changes in glacier area and volume over the simulation period. Area change is shown relative to the initial area, and in the case of the observed data point (blue; Fig. 8d), relative to observational estimates early in the 20th century. Consistent with the observation based findings of Jackson and Fountain (2007), rapid declines in area and volume (as inferred by observed thinning) occurred during warm and dry conditions early in the 20th century (Fig. 8c,d). During the 1950's to 1970's temperatures were cooler accompanied by higher precipitation (Fig. 8 a-c) which resulted in reduced rates of retreat and some advances and increases in glacier volume. After the mid-1970s, temperatures increased and precipitation decreased leading to more loss of area and volume. These periods of warm-dry and cold-wet conditions are attributed to phases of the Pacific Decadal Oscillation (Fig. 8a; PDO, Mantua et al. 1997) which have been shown to have a strong influence on glacier mass fluctuations (Bitz and Battisti, 1999; Moore and Demuth, 2001; Josberger et al., 2007). Over the historical period 1916-2004 the model predicted a 28% loss of glacier area which is within the range of uncertainty of the estimates of Jackson and Fountain (2007) who estimated a loss of a loss of 25 ± 10% for these glaciers (blue dot, Fig. 8; spatial changes are shown in Fig. 7). Glacier ice volume is more variable as it tracks precipitation variability, whereas glacier dynamics modulate the response of glacier area resulting in a more muted response to precipitation. Spikes in glacier area that do not correspond to spikes in glacier volume (e.g., early in the 21st century) indicate snow densification to ice outside of main glacier bodies during colder periods and do not indicate advances of large bodies of ice. Changes in volume do not always reflect changes in glacier area.

This is consistent with observations of Eliot Glacier volume by Jackson and Fountain (2007) who found that increased glacier thickness did not always correspond to gains in glacier area. This highlights the advantage of using a physical representation of glacier dynamics relative to simpler volume-area scaling approaches that are often used for glacier climatic response studies.

In the future period continued loss of glacier area and volume is predicted at nearly the same rate for both emissions pathway scenarios until about 2030. The loss of area and volume slows midcentury for scenario RCP4.5 reflecting a reduced rate of increasing temperature (Fig. 8a). The rate of volume and area loss decreases at 2075 under RCP8.5 when ice only remains at the highest elevations (above 2350 m). By the end of the 21st century, glacier area is projected to decrease 69 (59-81)% under RCP4.5 and 89 (80-96)% under RCP8.5, relative to the 2004 extent.

To evaluate how these changes in glacier area influence changes in dry season discharge we deconstructed long-term modeled discharge at the Eliot Creek diversion location, the water management location with the largest glacier contribution. Figure 9 shows 10-year centered mean modeled discharge volume from 1916-2099 during the entire dry season (July-Sept.; panels a,c) and during September only (panels b,d). Total discharge is plotted and is also separated into its sources: non-glacial (snowmelt + rain) and glacier melt. At this time of year most of the non-glacier component is from snowmelt. During the historical period the prominent pattern associated with PDO phases is clear. In cool-wet periods (e.g., 1945-1955; Fig 8a) there is high snowmelt and low glacier melt, while in warm-dry periods (e.g., 1925-1940; Fig 8a) there is less snowmelt and glacier melt increases. Historically, the interaction between these two discharge sources decreased variability in total discharge in response to variations in climate, demonstrating the buffering effect of glacier melt on streamflow. As the temperatures warmed after 1970 the amplitude of the snowmelt phases decreased and an overall negative trend dominates. In the future time period, decadal variability persists in the individual GCMs; however, it is not reflected in the ensemble mean because the timing of the decadal variability differs between GCM models. For July-Sept. discharge volume, sustained and slightly increasing glacier melt partially compensates losses of snowmelt; however, declines in glacier melt after 2010 further exacerbate the negative trend in total streamflow. For September flows the declining trend in glacier melt occurred earlier (1990) playing a more important role in declining water availability at this time of the year.

Fig. 10 expands this long term analysis to other locations in the basin. We plot the changes in dry season (July-Sept.) total discharge relative to the mean of dry season discharge for a reference period spanning 1916-1950. Changes in total discharge are expressed as a 10-year centered mean for clarity. Trends are negative across the basin, with the sharpest declines in the partially glacierized upland basins (Eliot and Coe Creek in the Middle Fork). In the ensemble mean for all of the locations, under RCP4.5 total discharge is predicted to decline 12-44% midcentury (2040-2060) and 14-63% late century (2080-2099). Under RCP8.5, total discharge is predicted to decline 13-49% midcentury and 18-78% late century. The largest declines in total runoff are expected in the upland drainages that experience losses in glacier area and that historically were more affected by seasonal snowmelt. The West Fork is the least sensitive basin as it had very little glacier contribution in the past and includes more low elevation area (Fig. 1) that is less sensitive to changes in snowmelt. Model streamflow projections for all locations represent natural, unregulated flow because the model does not represent water management effects. This assumption is important to consider when analyzing results for the downstream locations where upstream withdrawals and irrigation from diverted water and pumped groundwater change the water balance.

The relative glacier contribution to dry season flows expressed as a fraction of total flow is also shown in Figure 10 (green). At the headwater locations these fractions are predicted to increase until ~2040. However, at the Eliot Creek location glacier melt discharge volume is predicted to begin to decline around 2010 (Fig. 9). This increasing relative contribution despite declining glacier melt volume is the result of more rapid reductions in non-glacial sources of runoff. Despite decreasing melt volume the relative contribution of glacier melt remains high until mid-century at these headwater locations. Furthermore, as the seasonal snowpack date of disappearance shifts earlier in the year, the relative contribution of glacier melt increases earlier during the dry season. This increases the importance of glacier melt at times closer to the period of peak evapotranspiration (mid-July; Fig. 4) and maximum irrigation withdrawals. Historically glacier melt displayed the largest contribution after this period, late August through September.

We have demonstrated that over the historical time period natural multi-decadal variability plays a large role in determining changes in glacier melt and its contribution to dry season discharge. More subtle persistent changes resulting from glacier recession are modeled following climate warming. To highlight the importance of the period of analysis in investigations of changes in glacier contribution we calculated linear trends in glacier melt using multiple lengths of windows of analysis. We calculated linear trends in modeled glacier contribution to September discharge at the Eliot Creek location using the Sen's slope estimator (Sen, 1968) using 30, 40, 50, 60, and 70 year windows of analysis (Fig. 11). A single GCM scenario was used for the future period (bcc-cssm1-1). Trend significance was tested with the Mann Kendall tau statistic (Kendall, 1975) with statistical significance ($p<0.05$) denoted with filled circles. Using short periods of analysis (30-year) trend direction is much more sensitive to decadal variability; the direction can reverse depending on which period is analyzed due to strong natural variability (Fig. 8a). With the largest window length (70-year) a period of increasing contribution is identified followed by a persistent declining contribution (Fig. 11). This longer term analysis mutes the multi-decadal natural variability and the periods of initial flow augmentation through increased melt, peak contribution, and declining contribution are more clearly identified.

In most high elevation areas, records of hydrological and glaciological measurements rarely extend beyond several decades. For example, glaciers monitored by the National Park Service in the North Cascades region of Washington State began in the early 1990's. The longest record of glaciological measurements in the conterminous United States is for the USGS benchmark glacier, South Cascade, which began in the 1950's with discharge measurements starting in 1993. Even though this glaciological record is long, the period begins during a cool wet PDO phase and transitions to a warm dry PDO phase (Fig. 8a); hence trends would be largely influenced by the position of the time period amongst natural patterns of variability. This analysis highlights a challenge in determining changing contributions of glacier melt to discharge in areas with high natural climate variability and demonstrates a need for advanced observationally constrained simulation models for extending periods of analysis beyond the limits of observational records.

Our analyses have focused on the time of year when water demand is at its peak. The water resource infrastructure that was designed with reliance on available summer water may no longer be appropriate in a warmer climate. Given the projected decreases in water availability in the summer further analyses extended to all seasons can support the exploration of options for providing additional storage that will be needed (e.g., surface water storage, artificial aquifer recharge) and conservation measures (e.g., increased irrigation efficiency, improved surface water conveyance).

5. Conclusions

We have evaluated long-term changes in the contribution of glacier melt to the Hood River system using a spatially distributed hydrological model coupled with a glacier dynamics model. Our period of analysis spans 184 years from 1916 through 2099, which allows us to assess changes both in the period of almost 100 years during which observations are available, and through the remainder of the 21st Century (based on downscaled climate model projections). Our analysis shows that:

- Strong decadal variability in modeled glacier melt contribution is superimposed on declines linked to a long-term warming trend. Long time series of observed and modeled data are required to describe evolving glacio-hydrological processes in regions that experience pronounced natural climate variability.
- Supra-glacier debris cover plays a significant role on ablation rates retarding the retreat of glaciers. A comparison with a modeled debris-free condition showed that the reduced recession resulted in up to 14% more September discharge volumes, by the end of the historical period.
- The fraction of Hood River streamflow that originates as glacier melt is greatest in late summer in the headwater catchments, and ranges from 54% on average (maximum 79%) in the Eliot Creek basin to a much smaller 7% (maximum 24%) at the outlet of the basin.
- An ensemble of model simulations driven with projections of future climate indicate that dry season discharge (JAS) could decrease up to 78% by the end of the current century in headwater streams that were historically snow and ice melt dominated.

Our work highlights the relevance of dynamic process based glacio-hydrological modeling for future water management, land use, and conservation planning. The Hood River basin is one glacier fed system in the Pacific Northwest facing downstream risks posed by glacier recession with continued warming. Further modeling and observational studies are required to characterize and understand glacio-hydrological change for different river systems of varying environmental and climatic settings.

Acknowledgement:

We thank Matthew Bachmann, Howard Conway, and Andrew Fountain for their feedback after a presentation of this study, Niklas Christensen for providing naturalized stream flow data, and Stephen Burges for comments. This research was supported by the NASA Interdisciplinary Research in Earth Science Program - Grant NNX10AP90G.

References

Abatzoglou JT, Brown TJ. 2012. A comparison of statistical downscaling methods suited for wildfire applications. *International Journal of Climatology* **32**(5), 772-780. doi: 10.1002/joc.2312

Andreadis KM, Storck P, Lettenmaier D P. 2009. Modeling snow accumulation and ablation processes in forested environments. *Water Resources Research*, **45**(5).

Baraer M, Mark BG, McKenzie JM, Condom T, Bury J, Huh K, Portocarrero C, Gómez J, Rathay S. 2012. Glacier recession and water resources in Peru's Cordillera Blanca. *Journal of Glaciology* **58**, no. 207 (2012): 134-150.

Barnett TP, Adam JC, Lettenmaier DP. 2005. Potential impacts of a warming climate on water availability in snow-dominated regions. *Nature*, **438**(7066), 303-309.

Bitz CM, Battisti DS. 1999. Interannual to Decadal Variability in Climate and the Glacier Mass Balance in Washington, Western Canada, and Alaska. *Journal of Climate*, **12**(11), 3181-3196.

Bohn TJ, Livneh B, Oyler JW, Running SW, Nijssen B, Lettenmaier DP. 2013. Global evaluation of MTCLIM and related algorithms for forcing of ecological and hydrological models. *Agricultural and Forest Meteorology*, **176**, 38-49.

Brent RP. 1973. Chapter 4: An Algorithm with Guaranteed Convergence for Finding a Zero of a Function. In *Algorithms for Minimization without Derivatives*, Prentice-Hall: Englewood Cliffs, NJ, ISBN 0-13-022335-2

Casola JH, Cuo L, Livneh B, Lettenmaier DP, Stoelinga MT, Mote PW, Wallace JM. 2009. Assessing the Impacts of Global Warming on Snowpack in the Washington Cascades. *Journal of Climate*, **22**(10), 2758-2772.

Clark DH, Clark MM, Gillespie AR. 1994. Debris-covered glaciers in the Sierra Nevada, California, and their implications for snowline reconstructions. *Quaternary Research*, **41**(2), 139-153.

Clarke GKC, Anslow F, Jarosch A, Radic V, Menounos B, Bolch T, Berthier E. 2013. Ice volume and subglacial topography for western Canadian glaciers from mass balance fields, thinning rates, and a bed stress model. *Journal of Climate*, **26**(12), 4282-4303.

Clarke GKC, Jarosch A, Anslow F, Radic V, Menounos B. 2015. Projected deglaciation of Western Canada in the 21st century. *Nature Geoscience*, in press.

Coccoli H. 2002. Hood River Watershed Action Plan. Hood River Soil and Water Conservation District. June 19, 2002. Hood River, Oregon. 74 p.

Conway H, Rasmussen L.A. 2000. Summer temperature profiles within supraglacial debris on Khunibu Glacier, Nepal. In Debris-covered Glaciers: Proceedings of an International Workshop Held at the University of Washington in Seattle, Washington, USA, 13-15 September 2000 (No. 264, p. 89). IAHS.

Cuo L, Beyene TK, Voisin N, Su F, Lettenmaier DP, Alberti M, Richey JE. 2011. Effects of mid-twenty-first century climate and land cover change on the hydrology of the Puget Sound basin, Washington. *Hydrological Processes*, **25**(11), 1729-1753, doi: 10.1002/hyp.7932.

Daly C, Neilson P, Phillips DL. 1994. A statistical-topographic model for mapping climatological precipitation over mountainous terrain. *Journal of Applied Meteorology* **33**: 140–158.

Elsner MM, Cuo L, Voisin N, Deems JS, Hamlet AF, Vano JA, Mickelson K, Lee SY, Lettenmaier DP. 2010. Implications of 21st Century climate change for the hydrology of Washington State. *Climatic Change* **102**(1-2) 225-260, doi:10.1007/s10584-010-9855-0

Finger D, Pellicciotti F, Konz M, Rimkus S, Burlando P. 2011. The value of glacier mass balance, satellite snow cover images, and hourly discharge for improving the performance of a physically based distributed hydrological model. *Water Resources Research* **47**(7).

Fleming SW, Clarke GK. 2005. Attenuation of high-frequency interannual streamflow variability by watershed glacial cover. *Journal of Hydraulic Engineering*, **131**(7), 615-618.

Fountain AG, Tangborn WV. 1985. The effect of glaciers on streamflow variations. *Water Resources Research*, **21**(4), 579-586.

Hamlet AF, Lettenmaier D. P. 2005. Production of Temporally Consistent Gridded Precipitation and Temperature Fields for the Continental United States. *Journal of Hydrometeorology* **6**(3), 330-336.

Hock R, Jansson P, Braun LN. 2005. Modelling the response of mountain glacier discharge to climate warming. In Global Change and Mountain Regions (A State of Knowledge Overview)., Huber UM, Bugmann HKM, Reasoner MA (eds). Springer: Dordrecht; 243–252.

Immerzeel WW, Van Beek LP, Bierkens MF. 2010. Climate change will affect the Asian water towers. *Science* **328**(5984), 1382-1385.

Immerzeel WW, Van Beek LPH, Konz M, Shrestha AB, Bierkens MFP. 2012. Hydrological response to climate change in a glacierized catchment in the Himalayas. *Climatic change* **110**(3-4), 721-736.

Jackson KM. 2007. Spatial and morphological change of Eliot Glacier, Mount Hood, Oregon, Ph.D. dissertation, Portland State Univ., Portland, Oregon.

Jackson KM, Fountain AG. 2007. Spatial and morphological change on Eliot Glacier, Mount Hood, Oregon, USA. *Annals of Glaciology* **46**(1), 222-226.

Jarosch AH, Schoof CG, Anslow FS. 2013. Restoring mass conservation to shallow ice flow models over complex terrain. *The Cryosphere* **7**(1), 229-240.

Josberger EG, Bidlake WR, March RS, Kennedy BW. 2007. Glacier mass-balance fluctuations in the Pacific Northwest and Alaska, USA. *Annals of Glaciology* **46**(1), 291-296.

Jost G, Moore RD, Weiler M, Gluns DR, Alila Y. 2009. Use of distributed snow measurements to test and improve a snowmelt model for predicting the effect of forest clear-cutting. *Journal of Hydrology*, **376**(1), 94-106.

Jost G, Moore RD, Menounos B, Wheate R. 2012. Quantifying the contribution of glacier runoff to streamflow in the upper Columbia River Basin, Canada. *Hydrology and Earth System Sciences* **16**(3), 849-860.

Kampf, S. K., and S. J. Burges. 2007. A framework for classifying and comparing distributed hillslope and catchment hydrologic models, *Water Resources Research*, **43**, W05423, doi:10.1029/2006WR005370.

La Frenierre J, Mark BG. 2014. A review of methods for estimating the contribution of glacial meltwater to total watershed discharge. *Progress in Physical Geography* **38**(2), 173-200.

Lillquist K, Walker K. 2006. Historical glacier and climate fluctuations at Mount Hood, Oregon. *Arctic, Antarctic, and Alpine Research* **38**(3), 399-412.

Mantua NJ, Hare SR, Zhang Y, Wallace JM, Francis RC. 1997. A Pacific interdecadal climate oscillation with impacts on salmon production. *Bulletin of the American Meteorological Society* **78**(6), 1069-1079.

Meier MF. 1969. Glaciers and water supply. *Journal American Water Works Association* **61**: 8–12.

Mihalcea C, Mayer C, Diolaiuti G, Lambrecht A, Smiraglia C, Tartari G. 2006. Ice ablation and meteorological conditions on the debris-covered area of Baltoro glacier, Karakoram, Pakistan. *Annals of Glaciology* **43**(1), 292-300.

Moore RD, Demuth MN. 2001. Mass balance and streamflow variability at Place Glacier, Canada, in relation to recent climate fluctuations. *Hydrological Processes* **15**(18), 3473-3486.

Moore RD, Fleming SW, Menounos B, Wheate R, Fountain A, Stahl K, Holm K, Jakob, M. 2009. Glacier change in western North America: influences on hydrology, geomorphic hazards and water quality. *Hydrological Processes* **23**, 1: 42-61.

Moriasi DN, Arnold JG, Van Liew MW, Bingner RL, Harmel RD, Veith TL. 2007. Model evaluation guidelines for systematic quantification of accuracy in watershed simulations. *Transactions of the American Society of Agricultural and Biological Engineers* **50**(3), 885-900.

Naz BS, Frans CD, Clarke GKC, Burns P, Lettenmaier DP. 2014. Modeling the effect of glacier recession on streamflow response using a coupled glacio-hydrological model. *Hydrology and Earth System Sciences* **18**(2), 787-802.

Nolin AW, Phillippe J, Jefferson A, Lewis SL. 2010. Present-day and future contributions of glacier runoff to summertime flows in a Pacific Northwest watershed: Implications for water resources. *Water Resources Research* **46**(12).

Pelto MS. 2008. Impact of climate change on North Cascade alpine glaciers, and alpine runoff. *Northwest Science* **82**(1), 65-75.

Pelto MS. 2011. Skykomish River, Washington: Impact of ongoing glacier retreat on streamflow. *Hydrological Processes* **25**(21), 3356-3363.

Ragettli S, Pellicciotti F. 2012. Calibration of a physically based, spatially distributed hydrological model in a glacierized basin: on the use of knowledge from glaciometeorological processes to constrain model parameters. *Water Resources Research* **48**: 1–20. doi:10.1029/2011WR010559.

Reid TD, Brock BW. 2010. An energy-balance model for debris-covered glaciers including heat conduction through the debris layer. *Journal of Glaciology* **56**(199), 903-916.

Rupp DE, Abatzoglou JT, Hegewisch KC, Mote PW. 2013. Evaluation of CMIP5 20th century climate simulations for the Pacific Northwest USA. *Journal of Geophysical Research: Atmospheres*, **118**(19), 10-884.

Stahl K, Moore RD. 2006. Influence of watershed glacier coverage on summer streamflow in British Columbia, Canada. *Water Resources Research* **42**(6).

Stahl K, Moore RD, Shea JM, Hutchinson D, Cannon, AJ. 2008. Coupled modelling of glacier and streamflow response to future climate scenarios. *Water Resources Research*, **44**(2).

Steduto P, Hsiao TC, Fereres E, Raes D. 2012. Crop yield response to water. FAO irrigation and drainage paper, 66.

Taylor KE, Stouffer RJ, Meehl GA. 2012. An Overview of CMIP5 and the experiment design. *Bulletin of the American Meteorological Society* **93**(485-498) doi:10.1175/BAMS-D-11-00094.1.

Thornton PE, Running, SW. 1999. An improved algorithm for estimating incident daily solar radiation from measurements of temperature, humidity, and precipitation. *Agricultural and Forest Meteorology* **93**(4), 211-228.

Wigmosta MS, Vail LW, Lettenmaier DP. 1994. A distributed hydrology‐vegetation model for complex terrain. *Water Resources Research* **30**(6), 1665-1679.

Tables

Table 1: Model parameter values selected through calibration.

Parameter	Calibrated Value(s)
Precipitation Lapse Rate	2.5-15 [% 100 m^{-1}]*
Maximum Snow Albedo	0.8 [-]
Glacier Albedo	0.27 [-]
Lateral saturated hydraulic conductivity	1.0e-5 – 1.0e-3 [m sec^{-1}]*
Vertical Transmissivity Decay	2.0 [-]

*Spatially Variable

Table 2: CMIP5 general circulation model out used for projections of future climate under RCP4.5 and RCP8.5 emissions scenarios.

Model Name	Model Agency	Ensemble
bcc-cssm1-1	Beijing Climate Center, China Meteorological Administration	r1i1p1
CanESM2	Canadian Centre for Climate Modeling and Analysis	r1i1p1
CCSM4	National Center of Atmospheric Research, USA	r6i1p1
CNRM-CM5	National Centre of Meteorological Research, France	r1i1p1
CSIRO-Mk3-6-0	Commonwealth Scientific and Industrial Research Organization/Queensland Climate Change Centre of Excellence, Australia	r1i1p1
HadGEM2-CC	Met Office Hadley Center, UK	r1i1p1
IPSL-CM5A-MR	Institut Pierre Simon Laplace, France	r1i1p1
MIROC5	Atmosphere and Ocean Research Institute (The University of Tokyo), National Institute for Environmental Studies,and Japan Agency for Marine-Earth Science and Technology	r1i1p1
NorESM1-M	Norwegian Climate Center, Norway	r1i1p1

Table 3: Sensitivity (α) of the contribution of glacier melt to streamflow during September and July-September (shown in parentheses) period. The sensitivities represent the influence of parameter (θ) selection on modeled glacier contribution (mean 1916-2010). θ_0 represents the calibrated value where θ_{1-3} are incremented perturbations around the calibrated value.

	θ_0	θ_1	θ_2	θ_3	$\alpha_{\theta_0,\theta_1}$	$\alpha_{\theta_1,\theta_2}$	$\alpha_{\theta_2,\theta_3}$
Max. Snow Albedo [-]	0.80	0.81	0.82	0.83	-0.62 (-2.88)	-1.12 (-2.66)	-1.15 (-2.43)
Glacier Albedo [-]	0.27	0.26	0.28	0.29	0.2 (0.44)	-0.13 (-0.37)	-0.11 (-0.18)
Snow/Ice Roughness Length [m]	0.002	0.003	0.005	0.01	-0.01 (0.01)	0 (0.01)	0.01 (0.03)
Lateral saturated hydraulic conductivity	*	0.5Po	1.5Po	2Po	0.11 (0.09)	-0.32 (-0.25)	-0.06 (-0.05)

*Calibrated parameter values vary in space.

Table 4: Changes in seasonal precipitation and air temperature as projected by 9 statistically downscaled GCM outputs spatially aggregated across the basin. Changes in precipitation are shown as ratios while changes in temperature are shown as absolute values. The mean of 9 GCMs is reported while the range of the GCMs is denoted in parentheses.

Precipitation

	DJF	MAM	JJA	SON
1950-2005 (mm)	823	419	120	482
2040-2060 (RCP4.5)	1.06 (0.87-1.27)	1.02 (0.89-1.24)	0.86 (0.53-1.39)	1.01 (0.88-1.17)
2040-2060 (RCP8.5)	1.10 (0.84-1.32)	1.02 (0.77-1.23)	0.84 (0.46-1.20)	1.00 (0.83-1.27)
2080-2099 (RCP4.5)	1.09 (0.87-1.33)	0.99 (0.88-1.2)	0.86 (0.56-1.28)	1.03 (0.84-1.26)
2080-2099 (RCP8.5)	1.09 (0.89-1.27)	0.99 (0.82-1.19)	0.78 (0.42-1.19)	1.05 (0.88-1.32)

Temperature

	DJF	MAM	JJA	SON
1950-2005 ($°C$)	-0.2	5.4	14.7	7.8
2040-2060 (RCP4.5)	2.0 (1.2-2.9)	1.8 (1.2-2.5)	2.7 (1.6-3.9)	2.2 (1.2-3.1)
2040-2060 (RCP8.5)	2.4 (1.5-3.6)	2.1 (1.0-3.1)	3.4 (2.2-5.0)	2.9 (2.1-3.9)
2080-2099 (RCP4.5)	2.8 (1.6-3.9)	2.6 (2.1-3.3)	3.8 (2.6-5.1)	3.1 (2.2-4.3)
2080-2099 (RCP8.5)	4.6 (3.2-6.1)	4.2 (2.6-5.6)	6.7 (5.1-9.2)	5.4 (3.7-6.9)

Figures:

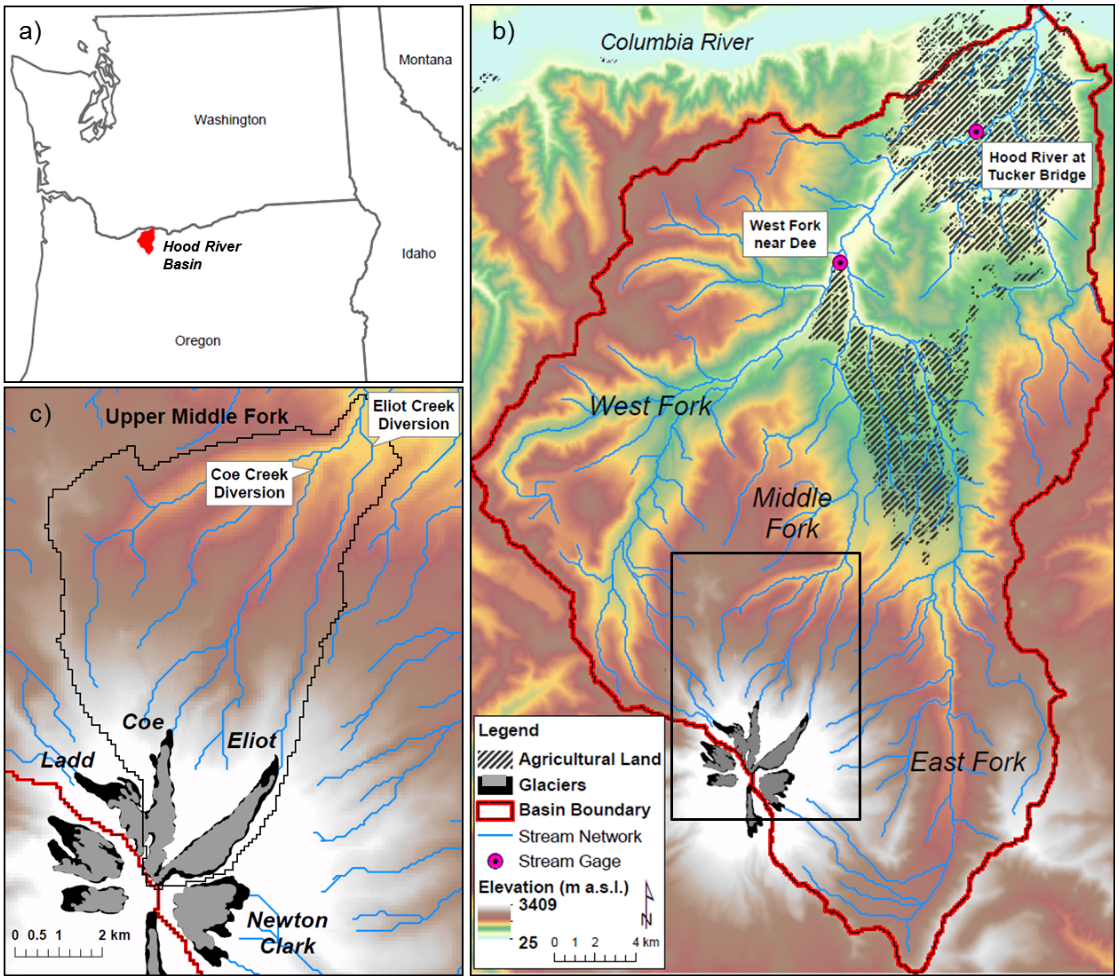

Figure 1: (a) Location of the Hood River Basin in NW Oregon U.S.A. (b) Depiction of the basin highlighting upstream tributaries, stream gauge locations, agricultural land, and Glacier area estimates of Jackson and Fountain (2007): ~1904 (black) and 2004 (gray). (c) the upper middle fork and water supply diversion locations.

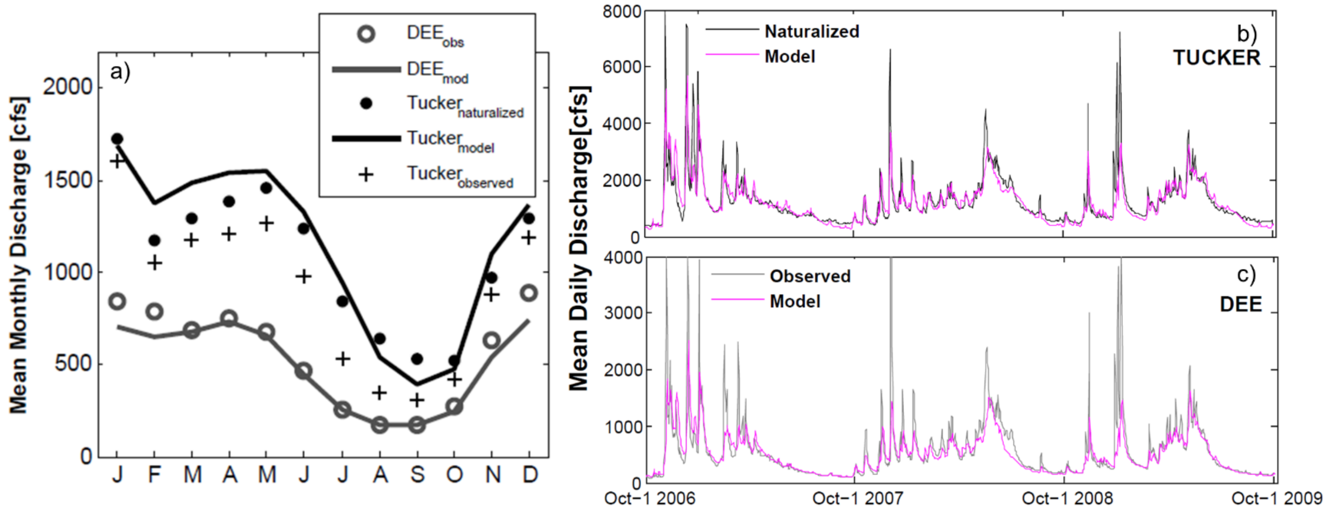

Figure 2: (a) Comparison of mean monthly observed and simulated streamflow (cubic feet second, cfs) for the West Fork of the Hood River near Dee, OR (WY 1933-2011), and at the Hood River at Tucker Bridge, where estimates of naturalized discharge are used for model calibration (WY 2002-2011). Naturalized, observed, and modeled discharge at the (b) Tucker and (c) Dee stream gauge locations at a daily time step for water years 2008-2010.

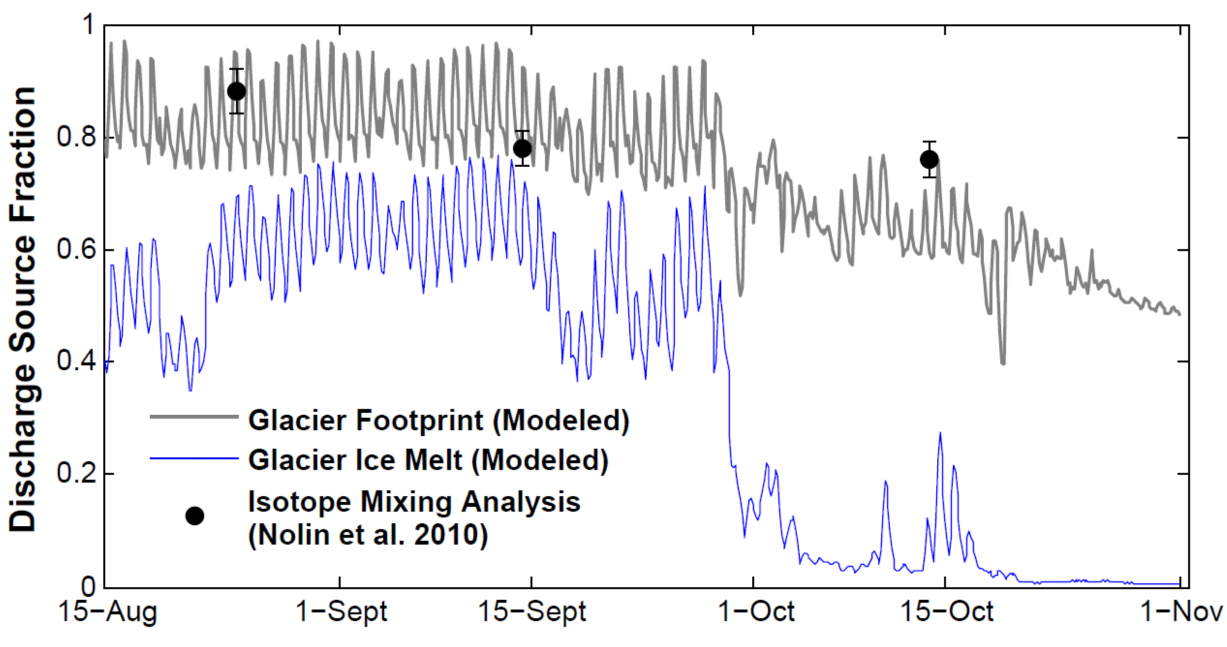

Figure 3: The modeled relative contribution of snowmelt, rain, and glacier melt from the footprint of Eliot glacier (gray) and from the melting of glacier ice only (blue) to downstream

discharge of Eliot Creek above the confluence with the Middle Fork at the end of the 2007 melt season. Estimates of the contribution from the glacier footprint from oxygen isotope sampling are plotted in black on each date of sampling (Nolin et al. 2010).

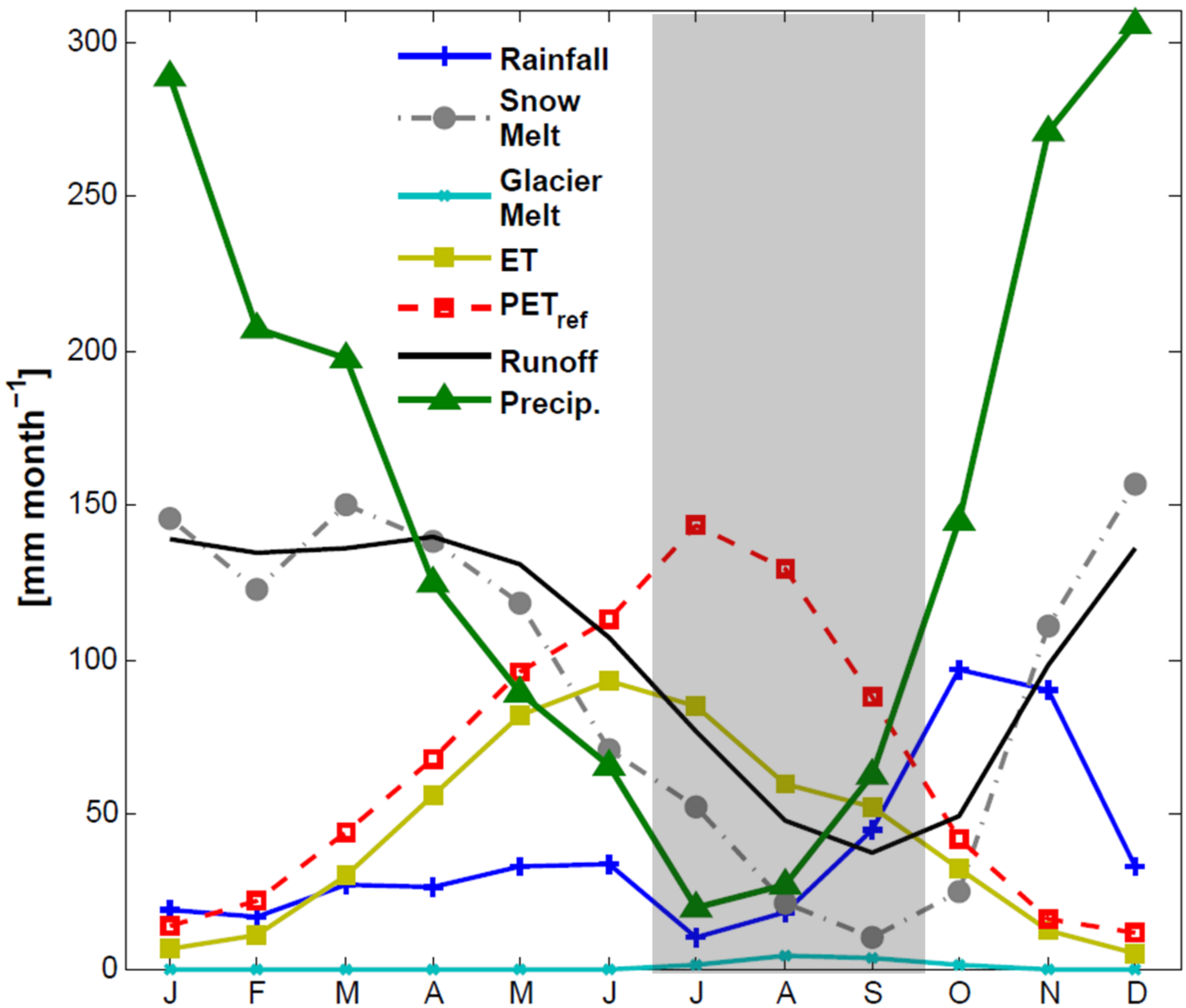

Figure 4: Modeled mean monthly hydrological fluxes spatially aggregated across the basin over the period of 1916-2005. The dashed box indicates a critical period where snowmelt and rain are at a minimum and soil moisture limitation is at maximum (as indicated by the difference between PET and ET).

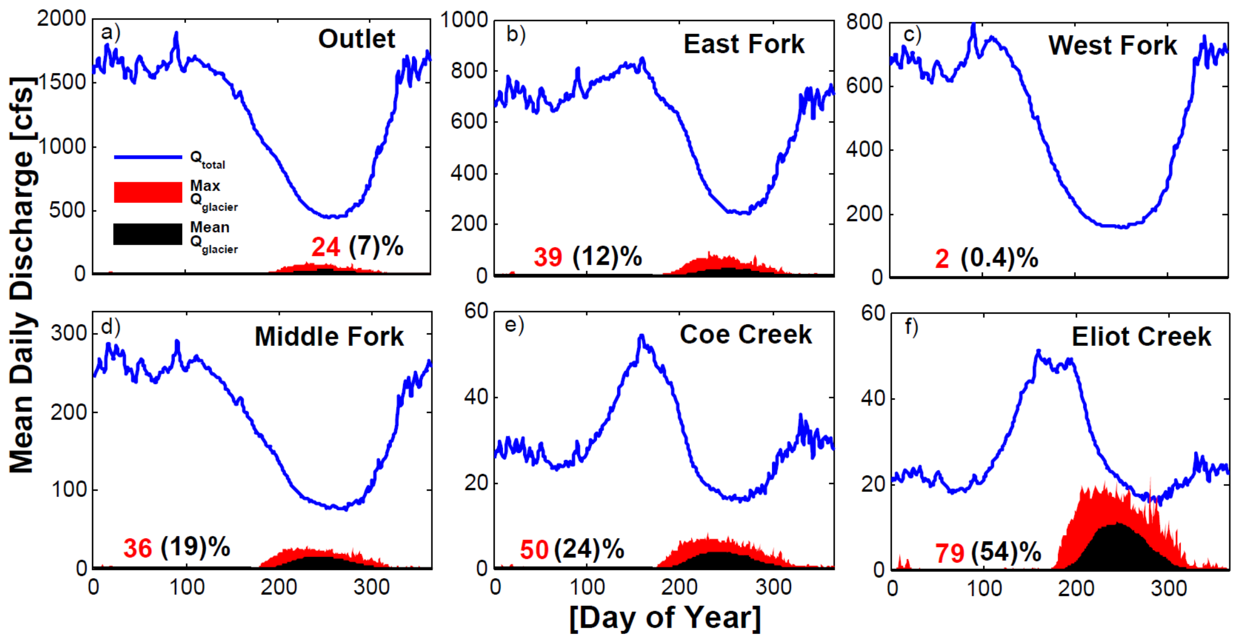

Figure 5: (a-f) Mean daily total discharge (blue), per day of year 1916-2005 for different stream locations in the basin (Fig. 1). Mean discharge from glacier melt is shown in black. The maximum daily mean discharge from glacier melt over the time period for each day is shown in red. The maximum daily contribution through the entire period is labeled with red text while the mean annual daily maximum glacier contribution is denoted with black text.

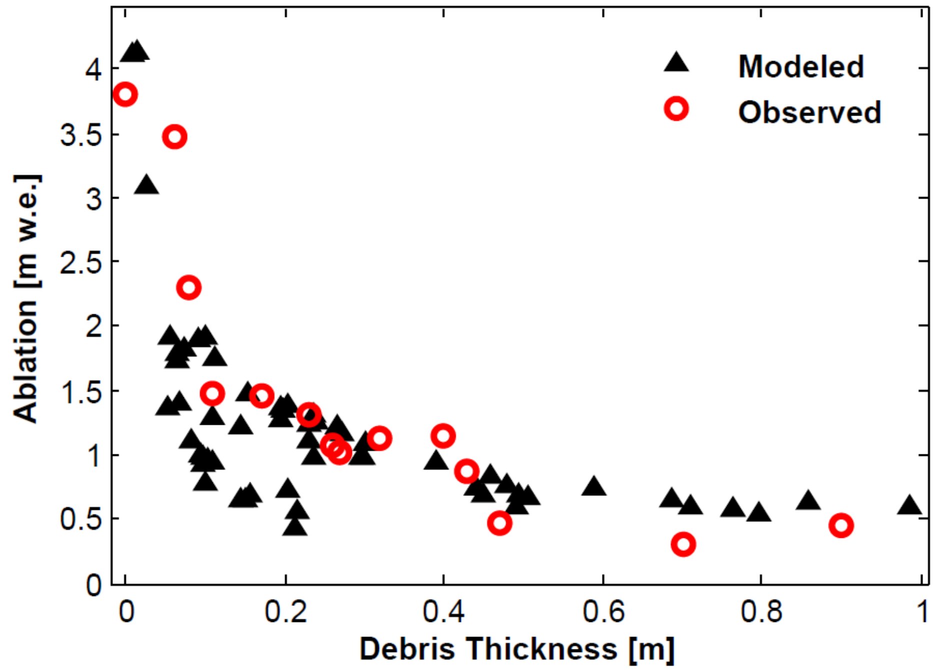

Figure 6: Observed and modeled ablation on the debris covered ablation area of Eliot glacier between 9-24-2004 and 7-28-2005 with varying range of debris thickness. Observations represent the ablation stake measurements of *Jackson and Fountain* [2007] while modeled values are presented for all debris covered grid cells on Eliot glacier.

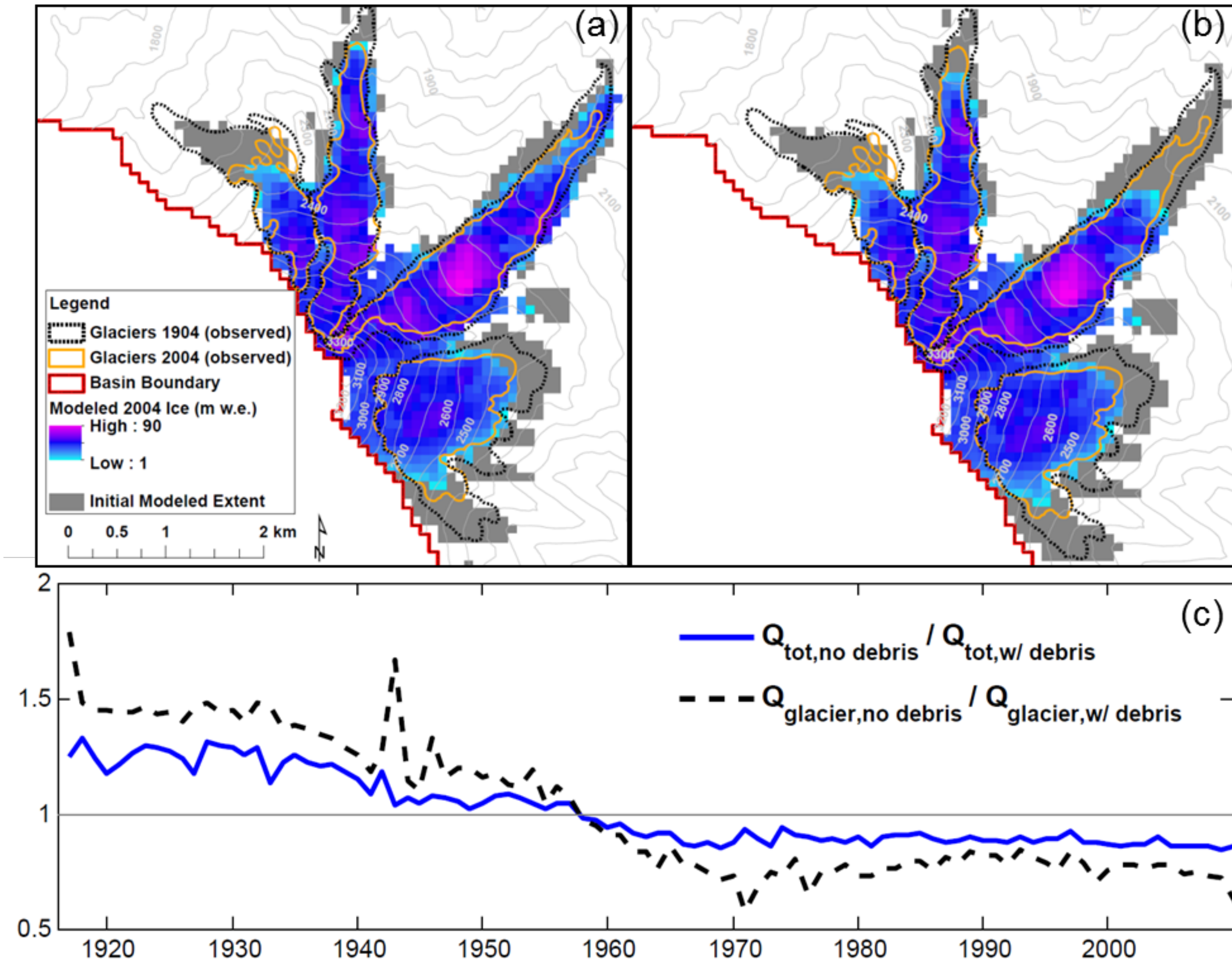

Figure 7: Experimental model simulations demonstrating the influence of surface debris on glacier area (a) with debris cover and (b) without debris at water year 2004. For reference outlines of historical estimates of glacier area from observations (Jackson and Fountain, 2007) are shown in addition to the initial extent used in the model simulations. (c) The progression of the ratio of modeled total discharge and glacier melt during the month of September using debris SEB algorithms to model results that do not consider debris is shown for the diversion location below Eliot glacier on Eliot Creek (Fig. 1).

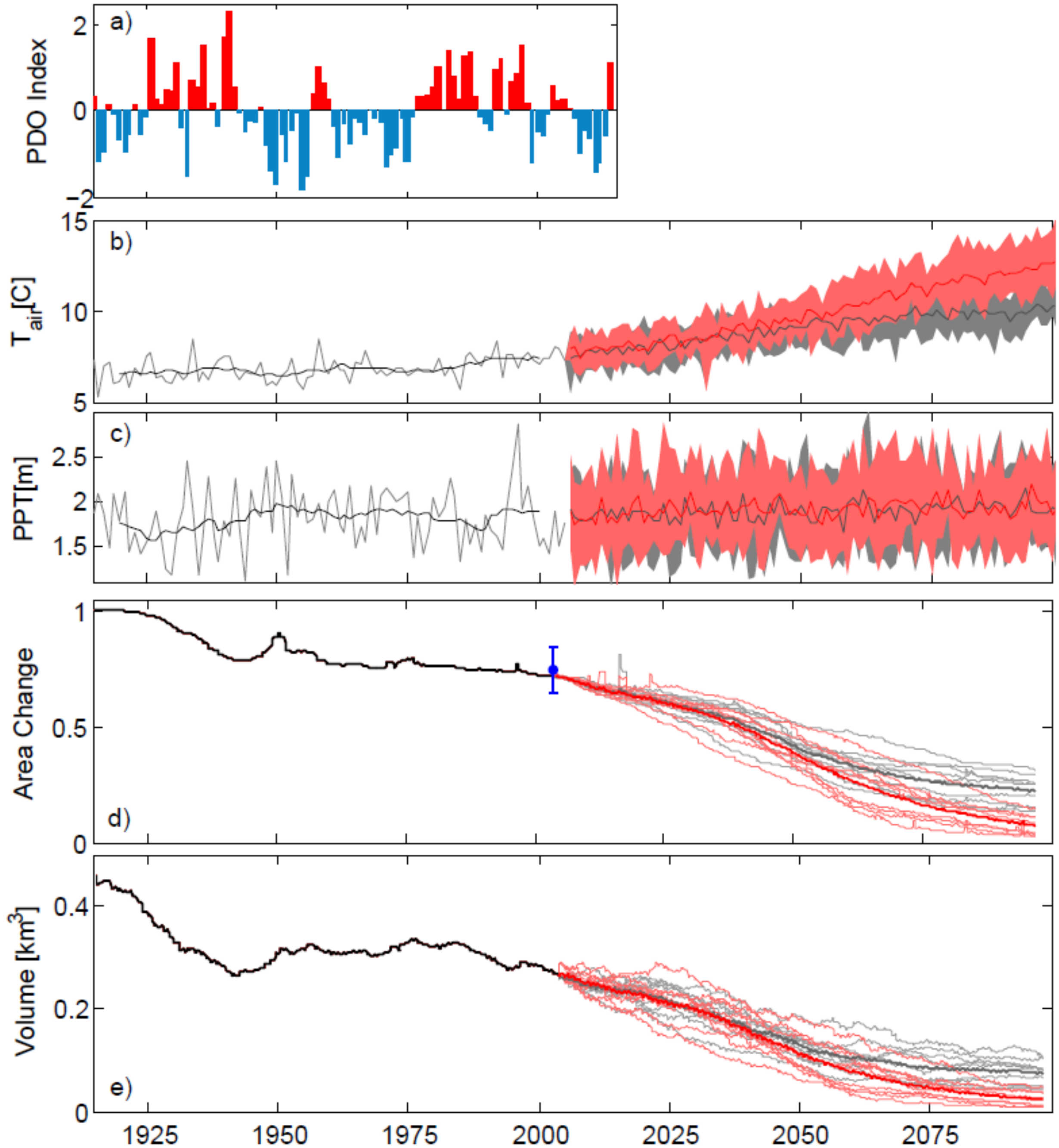

Figure 8: (a) Historical annual mean PDO Index (b) Mean annual temperature and (c) precipitation spatially aggregated across the basin. The black line denotes 10-year center mean over the historical period. In the future period the range of projections of RCP4.5 are indicated in gray and RCP8.5 in red while the dark lines denote the ensemble mean. Modeled progression of glacier (d) area (relative to initial area early in the 20th century) and (e) volume over this historical (black) and future RCP4.5 (gray), RCP8.5 (red) climate scenarios.

Observed estimates of glacier area change at 2004 (Jackson and Fountain, 2007) are indicated with the blue circle and whisker bars.

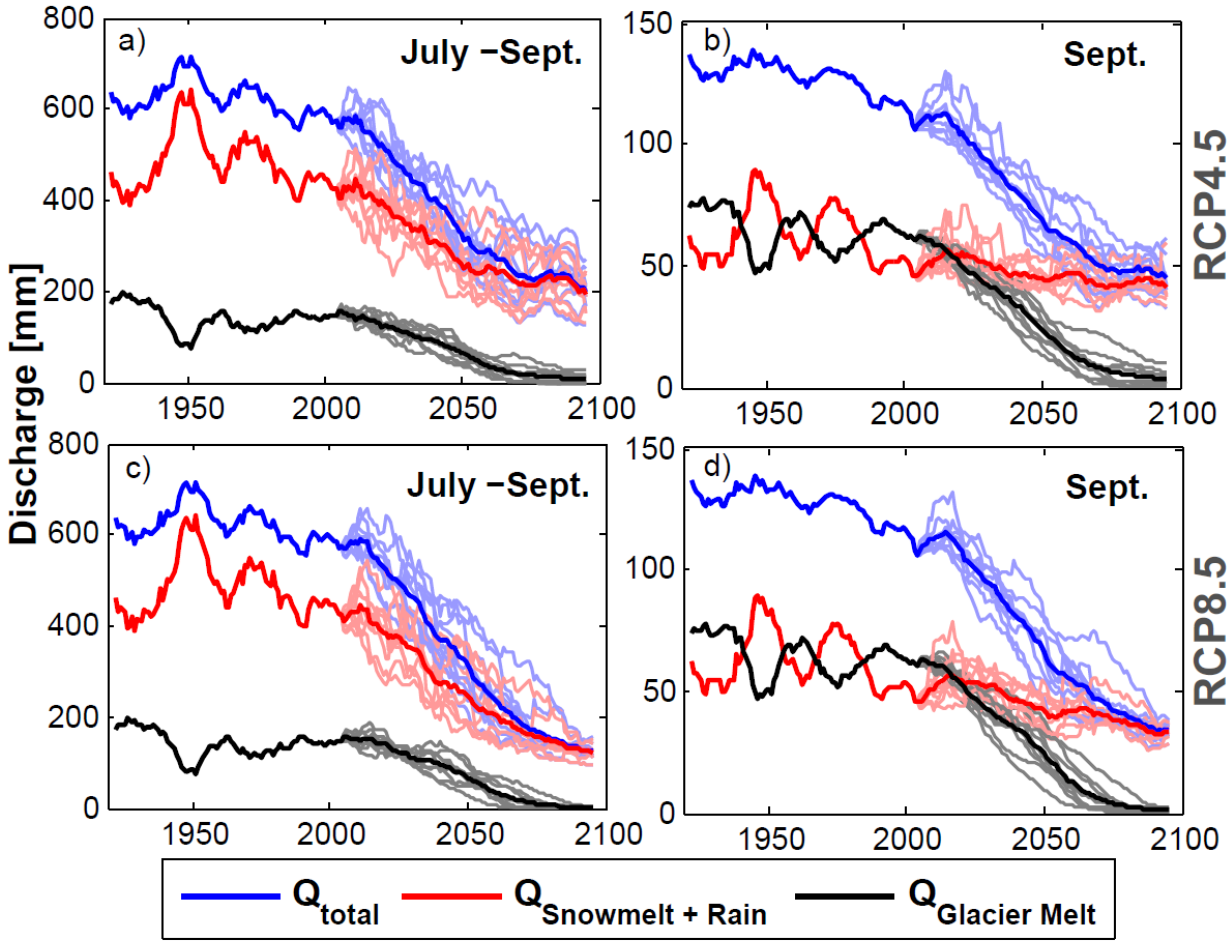

Figure 9: Historical and future (a,c) dry season (July – Sept) and (b,d) September discharge volume of Eliot Creek for CMIP5 (a,b) RCP4.5 and (c,d) RCP8.5 emissions scenarios.

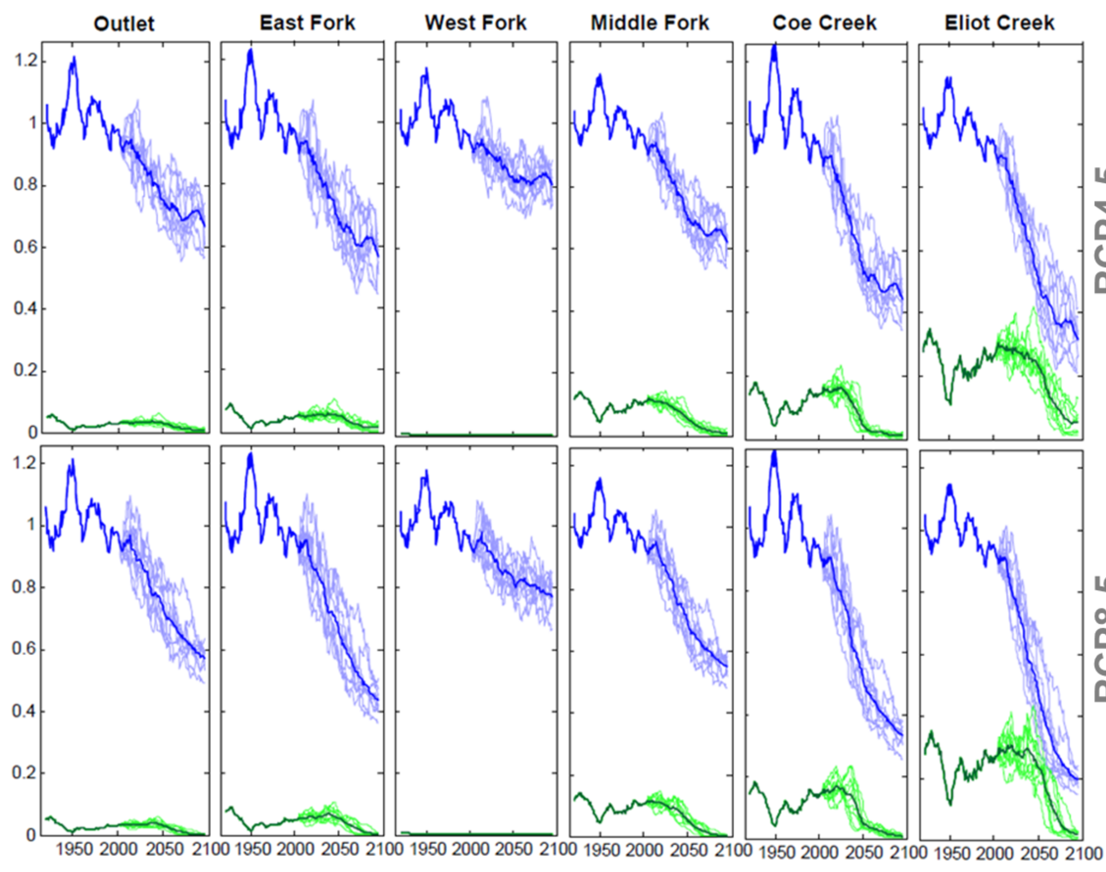

Figure 10: Projected changes in July-Sept. discharge volumes relative to the mean discharge for the period of 1916-1950 (blue) for the six locations in the basin. The relative glacier contribution to total discharge is plotted in green. Lighter colors indicate projections of individual GCMs where darker colors represent the ensemble mean and the historical period.

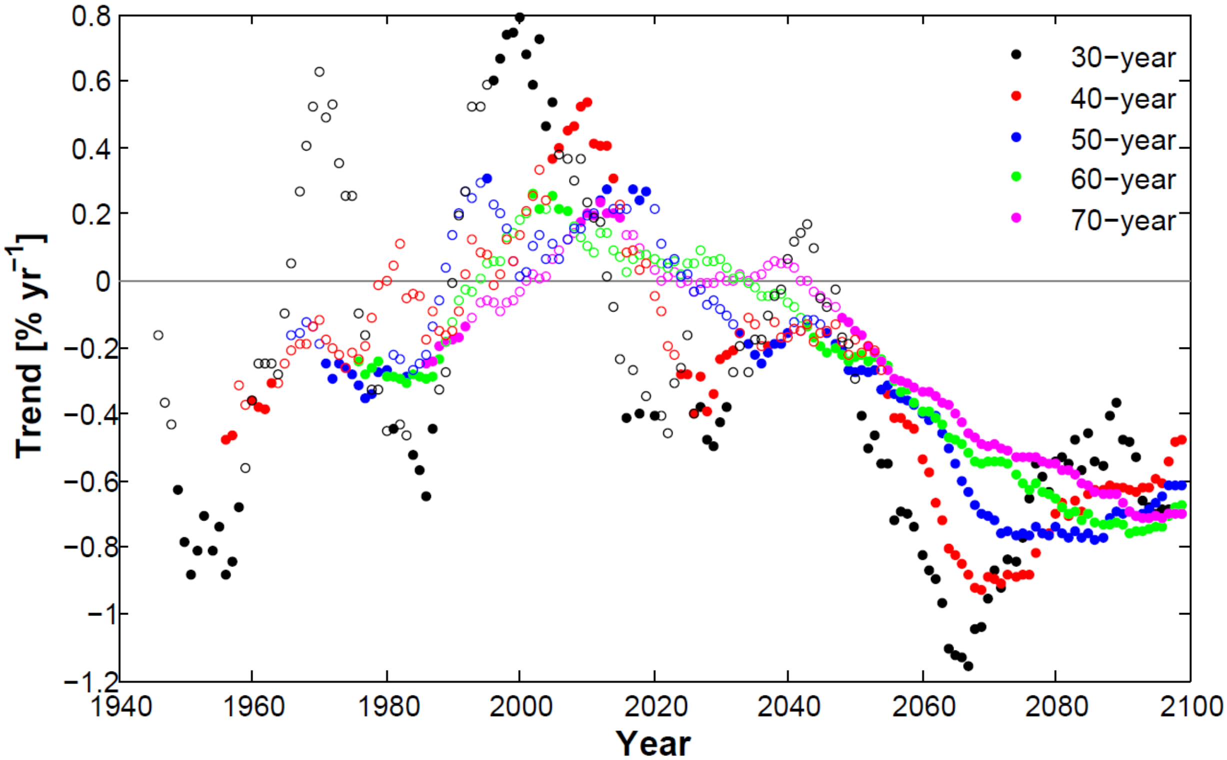

Figure 11: Linear trends in modeled Eliot creek September discharge volume using different length windows of analysis. Trend slope is reported as the Sen's slope estimator. Statistically significant trends ($p<0.05$) are denoted with filled symbols.